LITERATURE CITED

1. Amundson, N. R., *Can. J. Chem. Eng.*, **43**, 49 (1965).
2. Berger, A. J., and Leon Lapidus, *AIChE J.*, **14**, 558 (1968).
3. Bilous, O., and N. R. Amundson, *ibid.*, **1**, 513 (1955).
4. Chiou, J. K. S., and W. C. Cohen, paper presented at AIChE,, St. Louis meeting (1968).
5. Francis, J. G. F., *Computer J.*, **4**, 265, 332 (1961).
6. Hatfield, B., and Rutherford Aris, *Chem. Eng. Sci.*, **24**, 1213 (1969).
7. Levenspiel, O., "Chemical Reaction Engineering," Wiley, New York (1962).
8. Luss, D., and N. R. Amundson, *Chem. Eng. Sci.*, **22**, 253 (1967).
9. ——————, *Can. J. Chem. Eng.*, **45**, 341 (1967).
10. Luss, D., *Chem. Eng. Sci.*, **23**, 1249 (1968).
11. McGinness, P. H., Jr., *Chem. Eng. Progr. Symp. Ser. No.* **55**, **61** (1959).
12. McGowin, C. R., Ph.D. dissertation, Univ. Pennsylvania, Philadelphia (1969).
13. ———, and D. D. Perlmutter, *AIChE J.*, **17**, 837 (1971).
14. Perry, J. H., ed., "Chemical Engineers' Handbook," 4th edit., McGraw-Hill, New York (1963).
15. Raymond, L. R., and N. R. Amundson, *Can. J. Chem. Eng.*, **42**, 173 (1964).
16. Reilly, M. J., and R. A. Schmitz, *AIChE J.*, **12**, 153 (1966).
17. Van Heerden, C., *Ind. Eng. Chem.*, **45**, 1242 (1953).
18. ———, *Chem. Eng. Sci.*, **8**, 133 (1958).
19. Wehner, J. F., and Wilhelm, R. H., *ibid.*, **6**, 89 (1956).

II. Limiting Behavior and Collocation Solution of the Radial Mixing Case

A tubular reactor model that accounts for both radial gradients and nonflat velocity profile is unusually difficult to solve numerically, since even the steady state energy and material balances of the system are ordinarily coupled nonlinear partial differential equations. Nevertheless, techniques have been developed to obtain approximate or special-case analytical solutions. Kramers and Westerterp (*8*), von Rosenberg, Durrill, and Spencer (*14*), and Mickley and Letts (*11, 12*) used implicit finite-difference techniques to obtain direct numerical solutions. Hsu (*6*) obtained the analytical series solution of the material balance for the isothermal tubular reactor with finite radial mixing, parabolic velocity profile, first-order chemical reaction, and no axial diffusion, by reducing the system to an eigenvalue problem. The Taylor axial diffusion model (*1, 3, 15*) combines the effects of axial diffusion, radial concentration gradients, and parabolic velocity profile into a single axial diffusion term, reducing the steady state material balance for the isothermal system to a second-order ordinary differential equation. Deans and Lapidus (*4*) devised a two-dimensional array of interconnected continuous stirred-tank reactors to approximate the behavior of the packed-bed tubular reactor, and McGuire and Lapidus (*10*) used this model in an extensive numerical study to simulate the transient response of the system.

The model for the tubular reactor with finite radial mixing (TRRM) assumes that the velocity profile is flat, that axial diffusivity and conductivity are zero, and that heat transfer occurs across the reactor wall. The dimensionless steady state material and energy balances are

$$\frac{\partial y}{\partial z} = \frac{1}{N_{Pe'}} \frac{1}{r} \frac{\partial}{\partial r}\left[r \frac{\partial y}{\partial r}\right] - \mathcal{R}(y, \eta) \tag{1}$$

$$\frac{\partial \eta}{\partial z} = \frac{1}{N_{Pe}} \frac{1}{r} \frac{\partial}{\partial r}\left[r \frac{\partial \eta}{\partial r}\right] + \mathcal{R}(y, \eta) \tag{2}$$

and the boundary conditions are

$$z = 0: \quad y(0, r) = 1, \quad \eta(0, r) = \eta_F \tag{3}$$

$$r = 0: \quad \left.\frac{\partial y}{\partial r}\right|_0 = \left.\frac{\partial \eta}{\partial r}\right|_0 = 0 \tag{4}$$

$$r = 1: \quad \left.\frac{\partial y}{\partial r}\right|_1 = 0, \quad \left.\frac{1}{N_{Pe}} \frac{\partial \eta}{\partial r}\right|_1 = U_r\,[\eta_w - \eta(1)] \tag{5}$$

These boundary conditions assume flat radial concentration and temperature profiles at the reactor entrance and no mass transfer across the reactor wall. In the absence of radial velocity gradients, radial variations of concentration and temperature result from finite resistances to radial mass and heat transfer. Thus the radial heat and mass transfer Peclet numbers, N_{Pe} and $N_{Pe'}$, are computed using the thermal and mass diffusivities for the reactant mixture.

In the following, a direct comparison will be made of the collocation and implicit finite-difference techniques for obtaining solutions of Equations (1) and (2) numerically. In addition, limiting forms of this model will be explored analytically for both extremes of the degree of radial mixing.

LIMITING BEHAVIOR

As radial dispersive effects approach either zero or infinity in the tubular reactor system, the radial gradients of concentration and temperature must disappear when the entrance profiles and the velocity profiles are flat. This occurs at the zero mixing extreme, because there is no mechanism by which the uniform reaction effects can be redistributed; it must also be true when radial mixing is complete and all variations are averaged by mixing.

The limiting behavior may also be demonstrated analytically with the object of relating the TRRM parameters to those of the two limiting plug-flow tubular reactors. Assume that the chemical reaction is first order, irreversible, with Arrhenius temperature dependence:

$$\mathcal{R}(y, \eta) = k_0' \, y \exp(-\gamma/\eta) = k \, y \tag{6}$$

Then, for purposes of simplification, consider an isothermal TRRM with wall mass transfer. This system will exhibit linear kinetics by virtue of its isothermal character, yet it retains wall transfer analogous to that of the more general nonisothermal problem. Using a new concentration variable to emphasize the special character of this study, the material balance for the system is

$$\frac{\partial u}{\partial z} = \frac{1}{N_{Pe}} \frac{1}{r} \frac{\partial}{\partial r}\left[r \frac{\partial u}{\partial r}\right] - k\,u \tag{7}$$

and the corresponding boundary conditions are

$$z = 0: \quad u(0, r) = u_F \tag{8}$$

$$r = 0: \quad \left.\frac{\partial u}{\partial r}\right|_0 = 0 \tag{9}$$

$$r = 1: \quad \left.\frac{1}{N_{Pe}} \frac{\partial u}{\partial r}\right|_1 = k_w\,[u_w - u(1)] \tag{10}$$

The analytical solution of Equations (7) through (10) can be obtained using the finite Hankel transformation (see, for example, the text by Irving and Mullineux (7)) in the form

$$\frac{u}{u_w} = 1 + 2 \sum_{i=1}^{\infty} \left\{ \frac{\left[\frac{u_F}{u_w} - 1 + \mu_i\right] \exp\left[-\frac{kz}{\mu_i}\right] - \mu_i}{1 + \left[\frac{N_{Pe}\,k_w}{\lambda_i}\right]^2} \right\} \frac{J_1(\lambda_i) J_0(\lambda_i r)}{\lambda_i [J_0(\lambda_i)]^2} \tag{11}$$

The characteristic values λ_i in Equation (11) are roots of the equation

$$N_{Pe}\,k_w\,J_0(\lambda) = \lambda\,J_1(\lambda) \tag{12}$$

and the constants μ_i are functions of the corresponding value of λ_i

$$\mu_i = \frac{k}{(k + \lambda_i^2/N_{Pe})} \tag{13}$$

The characteristic values can be located by plotting the left and right sides of the following rearranged form of Equation (12):

$$\frac{J_0(\lambda)}{J_1(\lambda)} = \frac{\lambda}{N_{Pe}\,k_w} \tag{14}$$

simultaneously as functions of λ. The characteristic values λ_i are located at the points of intersection between the two sets of curves.

In the limit as radial mixing approaches zero and $N_{Pe} \to \infty$, the characteristic values λ_i approach the zeroes of $J_0(\lambda)$, and

$$\lim_{N_{Pe}\to\infty} \mu_i = 1 \tag{15}$$

$$\lim_{N_{Pe}\to\infty} \left[1 + \left(\frac{N_{Pe}\,k_w}{\lambda_i}\right)^2\right] [J_0(\lambda_i)]^2 = [J_1(\alpha_i)]^2 \tag{16}$$

where α_i is the i^{th} zero of $J_0(\lambda)$.

Using Equations (15) and (16) and the identity (7)

$$2 \sum_{i=1}^{\infty} \frac{J_0(\alpha_i r)}{\alpha_i J_1(\alpha_i)} = 1 \tag{17}$$

one finds the limiting form of Equation (11) to be

$$\lim_{N_{Pe}\to\infty} u(z, r) = u_F \exp(-kz) \tag{18}$$

Equation (18) is identical to the solution of the material balance equation for the isothermal plug-flow tubular reactor (PFTR):

$$\frac{du}{dz} = -ku + k_w'\,(u_w - u); \quad z = 0, \quad u(0) = u_F \tag{19}$$

when there is no mass transfer through the reactor wall ($k_w' = 0$).

In the limit as radial mixing approaches infinity and the radial Peclet number approaches zero, the characteristic values λ_i approach the zeroes of $J_1(\lambda)$, which are denoted by β_i. Since $\beta_1 = 0$ and $\beta_i > 0$ for $i > 1$

$$\lim_{N_{Pe}\to 0}\left[\frac{k}{\mu_i}\right] = \lim_{\substack{N_{Pe}\to 0\\ \lambda_i\to\beta_i}} \left(k + \frac{\lambda_i^2}{N_{Pe}}\right) = \begin{cases} k + \lim\limits_{\substack{N_{Pe}\to 0\\ \lambda_1\to 0}} \dfrac{\lambda_1^2}{N_{Pe}} & \text{for } i = 1 \\ \infty & \text{for } i > 1 \end{cases} \tag{20}$$

Thus all terms vanish in the series solution, Equation (11), except for the first term:

$$\lim_{N_{Pe}\to 0} \frac{u}{u_w} = 1 + \lim_{\substack{N_{Pe}\to 0\\ \lambda_1\to 0}} 2 \left\{ \frac{\left(\frac{u_F}{u_w} - 1 + \mu_1\right) \exp\left(-\frac{kz}{\mu_1}\right) - \mu_1}{1 + \left[\frac{N_{Pe}\,k_w}{\lambda_1}\right]^2} \right\} \frac{J_1(\lambda_1)\,J_0(\lambda_1 r)}{\lambda_1 [J_0(\lambda_1)]^2} \tag{21}$$

Rearrangement of Equation (12) yields

$$\frac{N_{Pe} k_w J_0(\lambda)}{\lambda} = J_1(\lambda) \tag{22}$$

which is used in conjunction with the identities

$$\lim_{\lambda\to 0} J_0(\lambda) = 1 \tag{23}$$

$$\lim_{\lambda\to 0} J_1(\lambda)/\lambda = 1/2 \tag{24}$$

to show that

$$\lim_{\substack{N_{Pe}\to 0\\ \lambda_1\to 0}} \left[\frac{k}{\mu_1}\right] = k + 2k_w \tag{25}$$

$$\lim_{\substack{N_{Pe}\to 0\\ \lambda_1\to 0}} \left[1 + \left(\frac{N_{Pe}\,k_w}{\lambda_1}\right)^2\right] = 1 \tag{26}$$

and

$$\lim_{\substack{N_{Pe}\to 0\\ \lambda_1\to 0}} J_0(\lambda_1 r) = 1 \tag{27}$$

Therefore, in the limit as radial mixing becomes infinite

$$\lim_{N_{Pe'}\to 0} u(z,r)$$

$$= \left[u_F - \frac{2k_w u_w}{k+2k_w} \right] e^{-(k+2k_w)z} + \frac{2k_w u_w}{k+2k_w} \quad (28)$$

Equation (28) is also the solution of the material balance equation for the isothermal plug-flow tubular reactor, Equation (19), when $k_w' = 2k_w$. In spite of the simplified form of Equation (7), it may be expected that the nonisothermal system represented by Equations (1) through (6) would behave similarly at the two extremes of radial mixing. As radial mixing approaches zero, the TRRM should reduce to an adiabatic PFTR ($U_r' = 0$), and in the limit as radial mixing becomes infinite, the TRRM should reduce to a nonadiabatic PFTR with $U_r' = 2U_r$. The heat transfer effect appears in two fundamentally different ways in the models for the TRRM and PFTR systems. In the radial mixing case, the wall boundary condition on temperature defines the rate of heat transfer, while in the plug-flow case, the heat transfer effect appears in the energy balance. Although the heat transfer coefficient has different meanings in the two systems, this analysis has shown that in the upper extreme of radial mixing, there is a rigorous relation between the two coefficients. Since the definitions of the dimensionless heat transfer coefficients differ by a factor of 2 in the two systems, the dimensional coefficients are numerically equal in the limiting case.

COLLOCATION AND FINITE-DIFFERENCE SOLUTIONS

The collocation method, a form of the method of weighted residuals (5), may be used to obtain approximate solutions of Equations (1) and (2). Trial solutions, containing known functions of radial position and several undetermined coefficients, are substituted for the dependent variables in the partial differential equations, and the error residuals that arise are set equal to zero at a series of m collocation points, distributed over the interval $0 < r < 1$. The result is a set of m ordinary differential equations (for each state variable of the system) in which the dependent variables are the undetermined coefficients in the trial solution.

Villadsen and Stewart (13) showed that it is also possible to write these reduced collocation equations directly in terms of the ordinates of the collocation points by expressing the Laplacian terms in Equations (1) and (2) in the form

$$\left.\frac{1}{r}\frac{\partial}{\partial r}\left(r\frac{\partial u}{\partial r}\right)\right|_{r_i} = \sum_{j=1}^{m+1} B_{ij}\, u(r_j) \quad (29)$$

The resulting collocation equations describe the behavior of y and η at each of the m interior collocation points as functions of axial position:

$$\frac{dy(r_i)}{dz} = \frac{1}{N_{Pe'}} \sum_{j=1}^{m+1} B_{ij}\, y(r_j) - \mathcal{R}(r_i) \quad i = 1, 2, \ldots, m \quad (30)$$

$$\frac{d\eta(r_i)}{dz} = \frac{1}{N_{Pe}} \sum_{j=1}^{m+1} B_{ij}\, \eta(r_j) + \mathcal{R}(r_i) \quad i = 1, 2, \ldots, m \quad (31)$$

The collocation constants B_{ij} are computed using the procedure described by Villadsen and Stewart (13). A series expansion in powers of r^2 is assumed for the dependent variable. This expansion satisfies the boundary conditions of the TRRM system at $r = 0$ automatically; however, the boundary conditions at $r = 1$ must be superimposed externally on the collocation equations. To do this, an extra collocation point (r_{m+1}) is placed at $r = 1$, the m^{th} collocation point is placed at $r_m = 1 - \delta r$, and finite-difference approximations are substituted for the gradient terms in the wall boundary conditions at $r = 1$:

$$r = 1, \quad \left.\frac{\partial y}{\partial r}\right|_1 = \frac{y(r_{m+1}) - y(r_m)}{\delta r} \quad (32)$$

$$\left.\frac{\partial \eta}{\partial r}\right|_1 = \frac{\eta(r_{m+1}) - \eta(r_m)}{\delta r} = N_{Pe} U_r\, [\eta_w - \eta(r_{m+1})] \quad (33)$$

The resulting collocation equations are

$$\frac{dy(r_i)}{dz} = \frac{1}{N_{Pe'}} \left[\sum_{j=1}^{m-1} B_{ij}\, y(r_j) + (B_{im} + B_{i,m+1})\, y(r_m) \right] - \mathcal{R}(r_i) \quad i = 1, 2, \ldots, m \quad (34)$$

$$\frac{d\eta(r_i)}{dz} = \frac{1}{N_{Pe}} \left[\sum_{j=1}^{m-1} B_{ij}\, \eta(r_j) + (B_{im} + aB_{i,m+1})\, \eta(r_m) + bB_{i,m+1} \right] + \mathcal{R}(r_i) \quad i = 1, 2, \ldots, m \quad (35)$$

To obtain the axial concentration and temperature profiles at each collocation point, Equations (34) and (35) are integrated numerically from $z = 0$ to $z = 1$, using the entrance conditions

$$z = 0: \quad y(0, r_i) = 1, \quad \eta(0, r_i) = \eta_F \quad i = 1, 2, \ldots, m \quad (36)$$

The implicit finite-difference techniques use finite-difference formulas to represent the gradient and Laplacian terms at a series of grid points, yielding a system of simultaneous algebraic equations. These are solved recursively for $y(z + \Delta z, r_i)$ and $\eta(z + \Delta z, r_i)$, given $y(z, r_i)$ and $\eta(z, r_i)$, until the axial concentration and temperature profiles at each grid point have been generated. Since the system of algebraic equations is nonlinear, Lee's quasilinearization algorithm (9), a modification of the Crank-Nicolson procedure (2), is useful. This technique transforms the computational problem from the solution of a large set of nonlinear algebraic equations to an iterative solution of a large set of linear algebraic equations.

NUMERICAL RESULTS

The collocation method and the quasilinearization method were each used to obtain numerical solutions of the TRRM steady state balances, Equations (1) and (2), for the set of parameters

$\eta_F = 3.50 \qquad U_r = 1$

$\eta_w = 3.25 \qquad \gamma = 60$

$N_{Pe'} = N_{Pe} = 25 \qquad k_0' = 1.0 \times 10^7$

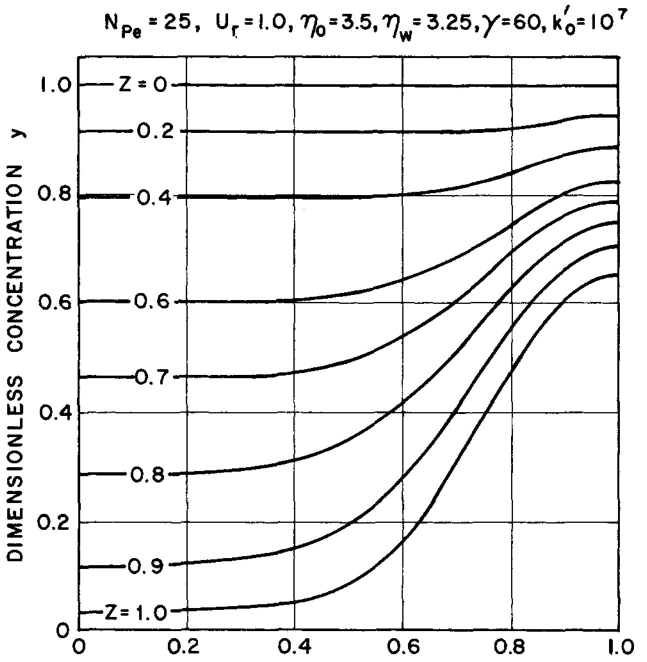

Fig. 1. Steady state concentration profiles for TRRM example.

In Figures 1 and 2 radial concentration and temperature profiles are plotted at several axial positions, distributed between the reactor entrance and exit. These profiles were generated using the quasilinearization method with a grid of 40 increments in the radial direction and 100 increments in the axial direction. The calculation was also performed using 20, 30, and 50 radial increments, and it was found that 40 finite-difference increments were needed to obtain agreement between successive degrees of approximation (to three significant figures).

The concentration and temperature profiles in Figures 1 and 2 clearly demonstrate the effects of radial mass and heat transfer resistance upon the concentration and temperature distribution in the reactor. A large radial temperature gradient develops downstream from the reactor entrance, resulting in much higher temperatures along the axis than along the wall of the reactor. This in turn causes a radial concentration gradient to develop, since the rate of depletion of reactant is higher along the reactor axis than along the wall.

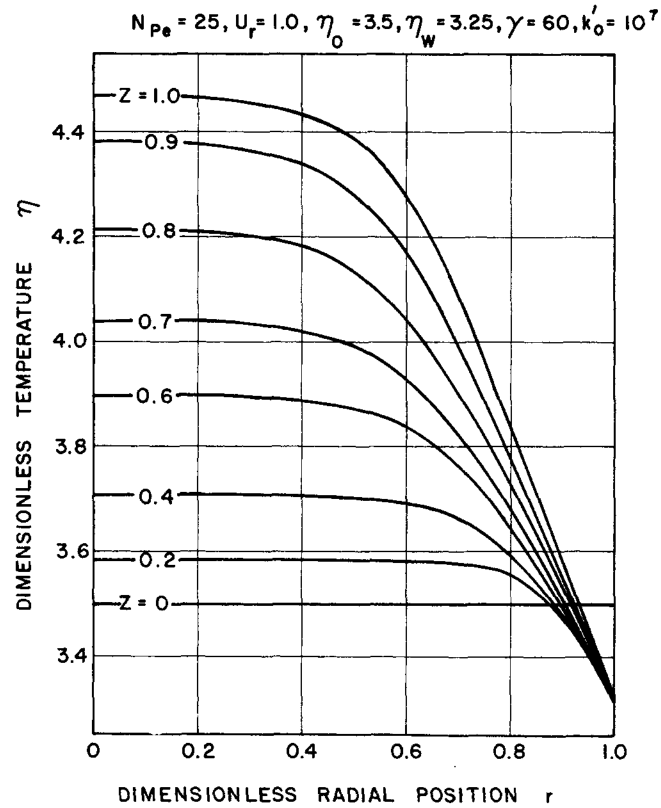

Fig. 2. Steady state temperature profiles for TRRM example.

In the collocation solutions, the collocation points were chosen arbitrarily, except for the points r_m and r_{m+1}, which were placed close together at the reactor wall ($r = 1$), as described earlier. The collocation constants were computed using the method outlined by Villadsen and Stewart (*13*), and are listed along with the collocation points in Table 1 for $m = 5$. The Runge-Kutta fourth-order formula was used to integrate the collocation equations over the length of the reactor, using a grid of 100 increments.

Table 2 compares the numerical solutions of the TRRM equations obtained using the collocation method with $m = 4$ and $m = 5$ collocation points and the quasilinearization method with 40 increments. The comparisons are made at the reactor exit ($z = 1$). There is excellent agreement between the solutions computed using the two meth-

TABLE 1. COLLOCATION POINTS AND CONSTANTS FOR TRRM-RECYCLE EXAMPLE
$m = 5$

Collocation points (r_i)

0.10	0.35	0.60	0.85	0.995	1.0

Collocation constants for radial Laplacian (B_{ij})

−55.151	69.324	−19.292	9.6228	−55.711	51.208
15.965	−46.920	37.349	−11.205	57.421	−52.610
−1.1347	20.069	−48.813	44.527	−160.686	146.038
7.6263	−22.589	54.040	−113.060	507.284	−433.301
−39.582	99.875	−138.777	353.068	−6176.718	5902.136
−48.913	122.933	−168.630	402.861	−6748.917	6440.664

Quadrature constants (W_i)

0.02545	0.07916	0.1643	0.1743	0.1774	−0.1207

ods, and the maximum difference is less than 2% of the feed stream conditions. Agreement between the collocation and quasilinearization solutions was slightly better for $m = 5$ than for $m = 4$ collocation points; however, collocation solutions obtained using $m = 2$ and $m = 3$ collocation points did not compare well with the finite-difference solution.

The quasilinearization solution obtained using 40 increments required the iterative solution of a set of 82 simultaneous nonlinear algebraic equations at each of the 100 axial grid points. The collocation solution obtained using five collocation points was of comparable accuracy, but it required only straightforward numerical integration of a set of 10 nonlinear ordinary differential equations from the entrance to the exit of the reactor. Thus it is evident that significantly fewer computations are required by the collocation method than by the quasilinearization method to yield a solution of comparable accuracy.

TABLE 2. COMPARISON OF COLLOCATION AND FINITE-DIFFERENCE SOLUTIONS OF STEADY STATE MATERIAL AND ENERGY BALANCES FOR TRRM

No. of collocation points	Axial position	Radial position	Concentration		Temperature	
m	z	r_i	y_{coll}	y_{FD}	η_{coll}	η_{FD}
4	1.0	0.30	0.04185	0.03997	4.452	4.454
		0.65	0.2291	0.2256	4.186	4.195
		0.90	0.6127	0.6078	3.561	3.578
		0.995	0.6622	0.6579	3.345	3.341
5	1.0	0.10	0.03303	0.03281	4.465	4.465
		0.35	0.04495	0.04512	4.446	4.446
		0.60	0.1591	0.1634	4.283	4.279
		0.85	0.5503	0.5494	3.705	3.706
		0.995	0.6705	0.6570	3.331	3.341

ACKNOWLEDGMENT

The authors gratefully acknowledge the support of the National Aeronautic and Space Administration, the family of Wilson S. Yerger, the National Science Foundation, and a University of Pennsylvania Computer Center grant of funds for computer time. Professor S. W. Churchill was most helpful as an interim advisor during Daniel D. Perlmutter's sabbatical leave.

NOTATION

a = $1/(1 + N_{Pe}\, U_r\, \delta r)$
b = $N_{Pe}\, U_r\, \eta_w\, \delta r/(1 + N_{Pe}\, U_r\, \delta r)$
B_{ij} = collocation constants for Laplacian
C = reactant concentration, g.-mole/cc.
C_p = fluid heat capacity, cal./(g.) (°K.)
D = radial mass diffusivity, sq.cm./sec.
E = activation energy, cal./g.-mole
$(-\Delta H_r)$ = heat of reaction, cal./g.-mole
$J_0(x)$ = zeroth order Bessel function
$J_1(x)$ = first-order Bessel function
k = first-order kinetic constant
k_w = dimensionless wall mass transfer coefficient
k_0 = frequency factor, sec.$^{-1}$
k_0' = dimensionless frequency factor $(k_0 L/v)$
L = reactor length, cm.
m = number of interior collocation points
N_{Pe} = radial heat transfer Peclet number $(vR'^2/\alpha L)$
$N_{Pe'}$ = radial mass transfer Peclet number (vR'^2/DL)
r = dimensionless radial position (r'/R')
r' = radial position, cm.
r_i = i^{th} collocation point
R = gas constant, 1.987 cal./(g.-mole) (°K.)
R' = reactor tube radius, cm.
$\mathcal{R}(y, \eta)$ = dimensionless reaction rate
$\mathcal{R}(r_i)$ = dimensionless reaction rate evaluated at the conditions at collocation point r_i
T = temperature, °K.
u = dependent variable in isothermal TRRM system
U = wall heat transfer coefficient, cal./(sq.cm.) (sec.) (°K.)
U_r = dimensionless wall heat transfer coefficient (TRRM: $UL/\rho C_p R'v$; PFTR: $2UL/\rho C_p R'v$)
v = flow velocity, cm./sec.
x = axial position, cm.
y = dimensionless reactant concentration (C/C_F)
z = dimensionless axial position (x/L)

Greek Letters

α = thermal diffusivity, sq.cm./sec.
α_i = i^{th} zero of $J_0(x)$
β_i = i^{th} zero of $J_1(x)$
γ = dimensionless activation energy $(\rho C_p E/(-\Delta H_r) C_F R)$
δ, Δ = linear difference operators
η = dimensionless temperature $(\rho C_p T/(-\Delta H_r) C_F)$
λ = characteristic value of isothermal TRRM equation
μ_i = $k/(k + \lambda_i^2/N_{Pe})$
ρ = fluid density, g./cc.

Superscript

$'$ = parameter of equivalent PFTR

Subscripts

F = evaluated at feed stream conditions
w = evaluated at wall conditions

LITERATURE CITED

1. Bischoff, K. B., *AIChE J.*, 14, 820 (1968).
2. Carnahan, B., H. A. Luther and J. O. Wilkes, "Applied Numerical Methods," preliminary edit., Wiley, New York (1964).

3. Coste, Rudd, D., and N. R. Amundson, *Can. J. Chem. Eng.*, **39,** 149 (1961).
4. Deans, H. A., and Leon Lapidus, *AIChE J.*, **6,** 656 (1960).
5. Finlayson, B. A., and L. E. Scriven, *Appl. Mech. Rev.*, **19,** 735 (1966).
6. Hsu, C. J., *AIChE J.*, **11,** 938 (1965).
7. Irving, J., and N. Mullineux, "Mathematics in Physics and Engineering," Academic Press, New York (1959).
8. Kramers, H., and K. R. Westerterp, "Elements of Chemical Reactor Design and Operation," Academic Press, New York (1963).
9. Lee, E. S., *Chem. Eng. Sci.*, **21,** 143 (1966).
10. McGuire, M. L., and Leon Lapidus, *AIChE J.*, **11,** 85 (1965).
11. Mickley, H. S., and R. W. M. Letts, *Can. J. Chem. Eng.*, **41,** 273 (1963).
12. *Ibid.*, **42,** (1964).
13. Villadsen, J. V., and W. E. Stewart, *Chem. Eng. Sci.*, **22,** 1483 (1967).
14. von Rosenberg, D. U., P. L. Durrill, and E. H. Spencer, *Brit. Chem. Eng.*, **7,** 186 (1962).
15. Wissler, E. H., *Chem. Eng. Sci.*, **24,** 527 (1969).

III. Effect of Recycle

This paper reports on an investigation of the individual effects of radial gradients and axial mixing on the steady state and stability characteristics of the tubular reactor-recycle system, differing in this respect from most previous studies which have concentrated on the case in which the reactor is a plug-flow tubular reactor (PFTR).

Bilous and Amundson (*2*) used Laplace domain techniques to show that unstable steady states are possible in the PFTR-recycle system. A thorough analysis of the PFTR-recycle system by Reilly and Schmitz (*9, 10*) showed that multiple steady states and unique unstable steady states are also possible. The transient behavior of the system was represented by a system of discrete equations, relating the reactant concentration and temperature of an element of fluid on its $(k+1)^{\text{th}}$ pass through the reactor exit to the conditions on the k^{th} pass through the exit.

Luss and Amundson (*5*) restricted their analysis to the adiabatic PFTR-recycle system, which allowed a graphical argument to be used to locate the steady states and determine their stability character. Root and Schmitz (*11*) investigated the adiabatic PFTR-recycle system experimentally and verified the presence of multiple steady states.

Schmeal and Amundson (*12*) solved the unsteady state material balance for an isothermal tubular reactor with axial mixing and recycle (TRAM-recycle). The analysis showed that the addition of a recycle line to the TRAM changes the character of the unsteady state response from nonoscillatory to oscillatory; that is, the dominant eigenvalue of the linear system changes from a real to a complex number.

THE TUBULAR REACTOR WITH RADIAL MIXING AND RECYCLE

The steady state material and energy balances and the boundary conditions of the tubular reactor with finite radial mixing were given in Part II (*8*):

$$\frac{\partial y}{\partial z} = \frac{1}{N_{Pe'}} \frac{1}{r} \frac{\partial}{\partial r}\left[r \frac{\partial y}{\partial r}\right] - \mathcal{R}(y, \eta) \tag{1}$$

$$\frac{\partial \eta}{\partial z} = \frac{1}{N_{Pe}} \frac{1}{r} \frac{\partial}{\partial r}\left[r \frac{\partial \eta}{\partial r}\right] + \mathcal{R}(y, \eta) \tag{2}$$

$$r = 0: \quad \left.\frac{\partial y}{\partial r}\right|_0 = \left.\frac{\partial \eta}{\partial r}\right|_0 = 0 \tag{3}$$

$$r = 1: \quad \left.\frac{\partial y}{\partial r}\right|_1 = 0, \quad \left.\frac{1}{N_{Pe}} \frac{\partial \eta}{\partial r}\right|_1 = U_r\left[\eta_w - \eta(1)\right] \tag{4}$$

An additional condition is needed at the reactor entrance in order to account for the recycle line. It is assumed that the recycle line is adiabatic, that no chemical reaction occurs outside the reactor, and that the recycle stream passes instantaneously from the exit to the entrance of the reactor, where it is instantaneously mixed with fresh feed. Inspection of the schematic flow diagram in Figure 1 shows that

$$z = 0: \quad y(0, r) = y_0 = (1 - R_r) + R_r \overline{y}(1) \tag{5}$$
$$\eta(0, r) = \eta_0 = (1 - R_r)\,\eta_F + R_r \overline{\eta}(1)$$

where $\overline{y}(1)$ and $\overline{\eta}(1)$ are the radial average concentration and temperature at the exit:

$$\overline{y}(1) = 2 \int_0^1 y(1, r)\, r\, dr \tag{6}$$

$$\overline{\eta}(1) = 2 \int_0^1 \eta(1, r)\, r\, dr \tag{7}$$

The last assumption—instantaneous recycle—is seldom satisfied in practice. Indeed, the presence of dead time in the recycle line can be a prime cause of instability in such

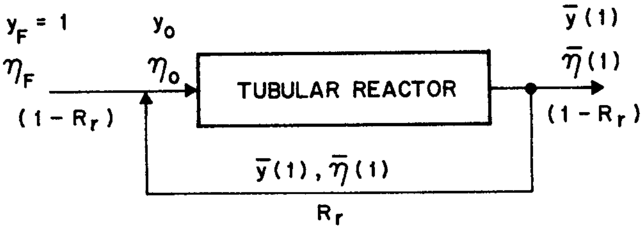

Fig. 1. Schematic diagram of tubular reactor recycle system.